

# The effect of vacuum annealing on graphene

Zhen Hua Ni,<sup>a</sup> Hao Min Wang,<sup>b</sup> Zhi Qiang Luo,<sup>a</sup> Ying Ying Wang,<sup>a</sup> Ting Yu,<sup>a</sup> Yi Hong Wu<sup>b</sup> and Ze Xiang Shen<sup>a\*</sup>

**The effect of vacuum annealing on the properties of graphene is investigated by using Raman spectroscopy and electrical measurement. Heavy hole doping on graphene with concentration as high as  $1.5 \times 10^{13} \text{ cm}^{-2}$  is observed after vacuum annealing and exposed to an air ambient. This doping is due to the H<sub>2</sub>O and O<sub>2</sub> adsorption on graphene, and graphene is believed to be more active to molecular adsorption after annealing. Such observation calls for special attention in the process of fabricating graphene-based electronic devices and gas sensors. On the other hand, because the quality of graphene remains high after the doping process, this would be an efficient and controllable method to introduce heavy doping in graphene, which would greatly help on its application in future electronic devices. Copyright © 2009 John Wiley & Sons, Ltd.**

**Keywords:** graphene; Raman spectroscopy; doping; annealing

## Introduction

Graphene exhibits excellent transport properties which make it a promising material for future nanoelectronic devices.<sup>[1,2]</sup> The large surface-to-volume ratio makes graphene extremely sensitive to the environment. The influence of the surroundings has been taken into account in many ways in the literature, such as the influence of substrate,<sup>[3,4]</sup> metal contacts<sup>[5]</sup> and shot noise.<sup>[6]</sup> Molecular doping of graphene has also attracted enormous interest.<sup>[7–12]</sup> It has been shown that the transport properties in graphene can be modified by adsorbing and desorbing gas molecules (NH<sub>3</sub>, NO<sub>2</sub>, CO, H<sub>2</sub>O).<sup>[8]</sup> To date, the direct impact of the surroundings during the fabrication of graphene-based devices is not fully understood. A better understanding of how graphene properties are expected to change during the fabrication of devices, such as by annealing, is highly required. On the other hand, characterizing the effects and avoiding/making use of them in device fabrication are also meaningful.

Raman spectroscopy has been historically used to probe structural and electronic characteristics of graphite materials, providing useful information on the defects (D band), in-plane vibration of sp<sup>2</sup> carbon atoms (G band) as well as the stacking orders (2D band).<sup>[13,14]</sup> Raman spectroscopy is also sensitive to the doping in graphene.<sup>[15–17]</sup> In this work, we demonstrate that graphene is heavily doped simply after annealing in vacuum and exposed to an air ambient. Hole concentration as high as  $1.5 \times 10^{13} \text{ cm}^{-2}$  is observed by Raman spectroscopy. Furthermore, the doping concentration is dependent on annealing temperature. We have also verified the doping effect by carrying out transport measurements in graphene before and after the vacuum annealing.

## Experimental

Graphene samples were prepared by micromechanical cleavage and transferred to an Si wafer with ~300-nm SiO<sub>2</sub> capping layer.<sup>[1]</sup> Optical microscopy was used to determine the thickness of graphene sheets, which was further confirmed by Raman and contrast spectroscopies.<sup>[18]</sup> High-temperature vacuum annealing

was carried out using a THMS 600 Linkam thermal stage with ~1 °C temperature accuracy and stability.<sup>[19]</sup> The vacuum of 0.5 Pa was achieved by a mechanical pump. The Raman spectra were recorded with a WITEC CRM200 Raman system with 532 nm (2.33 eV) excitation and with laser power at the sample below 0.5 mW to avoid laser-induced heating. A 50× long-working-distance (focal length = 10.1 mm) objective lens with NA = 0.55 was used in the *in situ* Raman measurement. For transport measurements, Au/Ti (30 × 10 nm) electrodes were directly evaporated onto selected single-layer graphene (SLG) flakes by using shield masks. The electrical transport properties of the devices were then measured before and after annealing by using a standard lock-in technique at room temperature. All the measurements were performed using a two-probe configuration under ambient conditions.

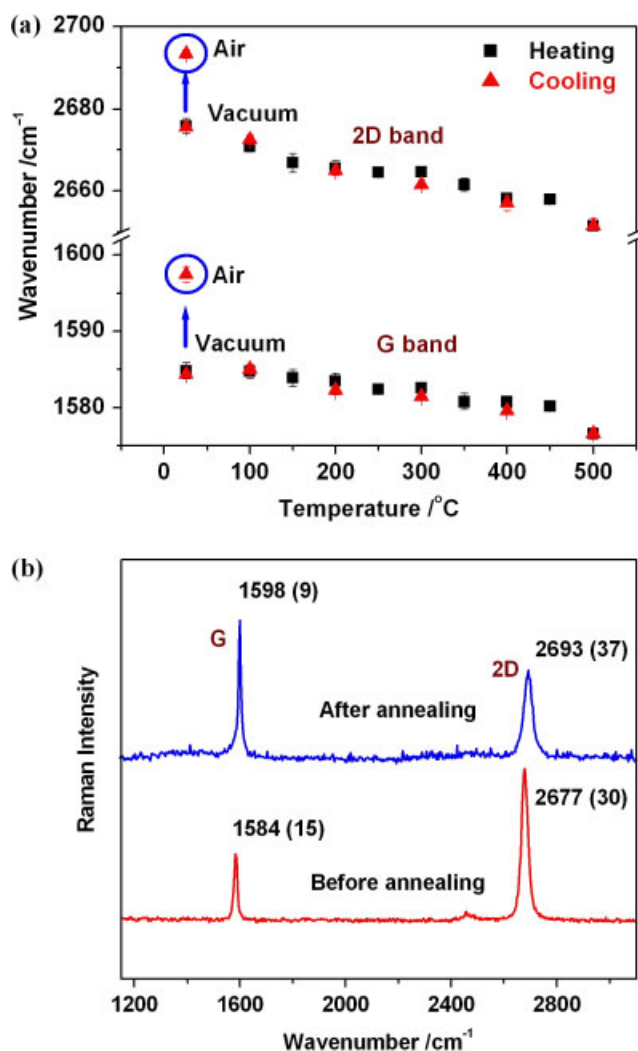
## Results and Discussion

Figure 1(a) shows the G and 2D band wavenumbers of SLG as the temperature was increased in the vacuum (black squares). The sample was heated up to 500 °C at 20 °C/min, and held for 10 min at every measurement point. The G and 2D band wavenumbers red shift at high temperature and the temperature coefficient is  $-0.019$  and  $-0.051 \text{ cm}^{-1}/^\circ\text{C}$ , respectively. Such phonon softening of graphene is due to the change of anharmonic potential constants, the phonon occupation number, as well as the thermal expansion at high temperature.<sup>[19]</sup> Among the three effects, the thermal expansion effect should be negligible as the thermal expansion coefficient of graphite/graphene is very small. Our result of the G

\* Correspondence to: Ze Xiang Shen, Division of Physics and Applied Physics, School of Physical and Mathematical Sciences, Nanyang Technological University, 21 Nanyang Link, Singapore 637371. E-mail: zexiang@ntu.edu.sg

a Division of Physics and Applied Physics, School of Physical and Mathematical Sciences, Nanyang Technological University, 21 Nanyang Link, Singapore 637371

b Department of Electrical and Computer Engineering, National University of Singapore, 4 Engineering Drive 3, Singapore 117576



**Figure 1.** (a) The G and 2D band frequencies of SLG with temperature increases to 500 °C (squares) and cools down to room temperature (triangles). The arrows indicate the change of Raman bands when graphene is exposed to air ambient after vacuum annealing. (b) The Raman spectra of graphene before and after vacuum annealing and exposed to air ambient. The numbers above each indicate the peak wavenumber and bandwidth.

band temperature coefficient ( $-0.019 \text{ cm}^{-1}/^{\circ}\text{C}$ ) of SLG is slightly larger than that obtained by Calizo *et al.*<sup>[20]</sup> ( $-0.016 \text{ cm}^{-1}/^{\circ}\text{C}$ ) in the temperature range between  $-190$  and  $100^{\circ}\text{C}$ . This is because the temperature-induced Raman shift is not linear across the whole temperature range, with a larger shift at higher temperatures.<sup>[21]</sup>

After reaching the highest temperature of  $500^{\circ}\text{C}$ , the sample is cooled down to room temperature (red squares) and the Raman bands blue-shift back to the same wavenumbers as before annealing and exposure to an air ambient. Interestingly, after opening the vacuum chamber and exposing the graphene to the air ambient, the G and 2D band wavenumbers show a sudden blue shift of  $14$  and  $16 \text{ cm}^{-1}$ , respectively, as shown by the blue arrows in Fig. 1(a). Figure 1(b) shows the Raman spectra of graphene before and after annealing. The blue shift of G and 2D bands are very obvious. This blue shift is unlikely to be due to the compressive stress on graphene by substrate,<sup>[22]</sup> as there is no thermal expansion at room temperature, which is necessary to cause the stress. Moreover, the stress-induced blue shift of the 2D band wavenumber should be  $\sim 2$  times greater than the G band

wavenumber,<sup>[22]</sup> which is inconsistent with our observation. On the other hand, the observed phenomena are coincident with what has been observed in the hole doping of graphene with electrical field applied by gate voltage.<sup>[17]</sup> The electron/hole doping in graphene will affect the interaction between optical phonons and the Dirac fermion transitions across the zero bandgap of semimetallic graphene. Hence, at strong electron/hole doping, the G band phonon shows a stiffening as well as narrowing of the bandwidth.<sup>[23]</sup> The stiffening of the G peak is due to the nonadiabatic removal of the Kohn anomaly at  $\Gamma$  point. The bandwidth narrowing is due to blockage of the phonon decay into electron–hole pairs due to the Pauli exclusion principle. In our case, after vacuum annealing and exposure to air ambient, the G band wavenumber of SLG has a blue shift of  $\sim 14 \text{ cm}^{-1}$ , and its bandwidth changes from  $15$  to  $9 \text{ cm}^{-1}$ . This is in accordance with the doping effect. For the 2D peak, the influence of dynamic effects is expected to be negligible, since the 2D phonons are far away from the Kohn anomaly at  $K$  point. Therefore, the effect of doping on the 2D band is mainly due to the charge-transfer-induced modification of the equilibrium lattice parameter with a consequent stiffening/softening of the phonons, with hole doping resulting in a blue shift, and the opposite is true for electron doping.<sup>[17]</sup> In our sample, the 2D band blue shifts by  $\sim 16 \text{ cm}^{-1}$ , which indicates that the graphene sample is strongly hole-doped after vacuum annealing and exposure to air ambient. Compared to the results in the electrical field-induced doping,<sup>[17]</sup> the hole doping in our sample is  $\sim 1.5 \times 10^{13} \text{ cm}^{-2}$ .

The doping is most likely caused by the molecular adsorption on graphene, and the consequent charge transfer between the molecules and graphene.<sup>[8,10]</sup> Previous experiment on the transport measurement of graphene has demonstrated the increase in graphene charge carrier concentration induced by adsorbed gas molecules ( $\text{NH}_3$ ,  $\text{NO}_2$ ,  $\text{CO}$ ,  $\text{H}_2\text{O}$ ).<sup>[8]</sup> According to that result, the adsorbed  $\text{H}_2\text{O}$  and  $\text{NO}_2$  molecules work as acceptors, whereas  $\text{NH}_3$  and  $\text{CO}$  work as donors.  $\text{O}_2$  is also a well-known electron acceptor.<sup>[24]</sup> Before the vacuum annealing, there should be  $\text{H}_2\text{O}$  and  $\text{O}_2$  molecules adsorbed on graphene.<sup>[25]</sup> However, the amount is small and the doping effect is weak, which is confirmed by the close G band wavenumber of the pristine graphene ( $1581\text{--}1584 \text{ cm}^{-1}$ ) compared to the undoped graphene ( $1581 \text{ cm}^{-1}$ ).<sup>[23]</sup> We believe that, after high-temperature vacuum annealing, the  $\text{H}_2\text{O}$  and  $\text{O}_2$  molecules in air can adsorb on graphene much more easily, which introduce strong doping in graphene. After annealing, the adsorbates on graphene are much reduced,<sup>[26,27]</sup> which provide adsorption sites for  $\text{H}_2\text{O}$  and  $\text{O}_2$  molecules. Transmission electron microscopy (TEM) results also show that graphene is extremely lipophilic after annealing, and attracts a thin layer of molecules after being exposed in air.<sup>[27]</sup> The  $\text{H}_2\text{O}$  and  $\text{O}_2$  molecules are not from the  $\text{SiO}_2$  substrate, as no doping effect is observed before graphene is exposed to air ambient, as shown later in step 2 of Fig. 2. We have tried to anneal the sample and subject it to a pure  $\text{N}_2$  atmosphere, but no changes in Raman spectra were observed. This partially supports the above conclusion that  $\text{H}_2\text{O}$  and  $\text{O}_2$  in ambient air is the main source of doping in graphene. It is also worth noting that after the vacuum annealing and exposure to air ambient, there is no disorder-induced D band at  $\sim 1350 \text{ cm}^{-1}$  in the Raman spectrum of SLG (Fig. 1(b)). This suggests that the sample is still of high quality after the annealing. This is important, as the quality of graphene will affect its transport properties greatly. The annealing of graphene in  $\text{O}_2$  has also been reported recently.<sup>[28]</sup> It revealed that graphene is etched in the  $\text{O}_2$  atmosphere and etch pits of tens

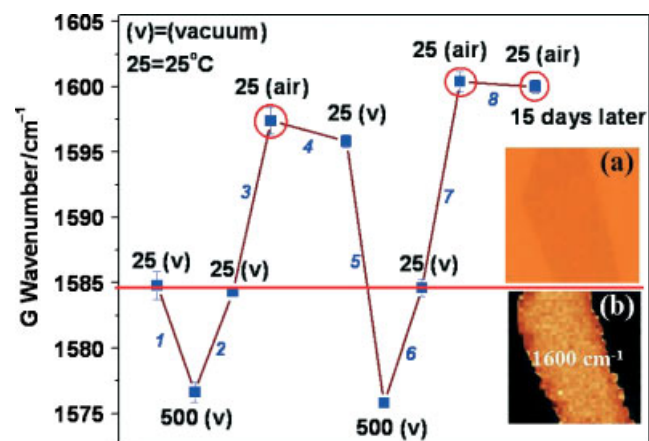


**Figure 2.** The doping process of SLG. Graphene sample is heated to 500 °C in vacuum (step 1), and cooled down to room temperature (step 2), then exposed to air ambient (step 3). To check the stability, sample is introduced into vacuum for 2 h (step 4). It is then heated again to 500 °C (step 5) and cooled down (step 6), exposed to air ambient (step 7). The sample is checked after leaving in air for 15 days (step 8). The doping molecules are stable in air and vacuum and can be removed after vacuum annealing. Inset (a) shows a SLG sample and inset (b) shows the G band wavenumber imaging of the sample after annealing and doping. The imaging indicates that the molecular doping is uniform across the whole sample.

of nanometers can be found across the sample. At the same time, disorder-induced D band can be obviously seen on the annealed sample.

To check whether the adsorbed molecules are stable, we introduced the sample into vacuum again for 2 h. The results are shown in Fig. 2. Only a slight red shift (1–2  $\text{cm}^{-1}$ ) of the G band is observed (step 4 in Fig. 2), which suggests that the molecules are stable even under vacuum conditions. Following this, we re-annealed the sample at 500 °C for 30 min (step 5 in Fig. 2) and cooled it to room temperature of 25 °C (step 6 in Fig. 2). The G band shifts back to original position as before annealing, indicating that adsorbed molecules are removed by high-temperature annealing. However, after exposing graphene to air, the G band blue shift of 16  $\text{cm}^{-1}$  is again observed (step 7 in Fig. 2), indicating the re-adsorption of  $\text{H}_2\text{O}/\text{O}_2$  molecules. The larger amount of blue shift in step 7 compared to step 3 (14  $\text{cm}^{-1}$ ) is due to the overall longer time of annealing, which introduces more doping in graphene. Note that the amount of blue shift is almost unchanged even after 15 days in air (step 8 in Fig. 2). Therefore, the adsorbed molecules are stable in air and vacuum and can only be removed after high-temperature vacuum annealing. The inset (a) of Fig. 2 shows a SLG sample and inset (b) shows the Raman imaging constructed by the G band wavenumber of the same sample after annealed at 500 °C and exposed to air. The G band wavenumber is at  $\sim 1600 \text{ cm}^{-1}$  across the whole sample. This suggests that the molecular doping on graphene is uniform.

Following this, graphene was annealed at different temperatures in vacuum, cooled down and then exposed to air ambient. The blue shifts of the G band of SLG after annealing at different temperatures are shown in Fig. 3. The Raman bands of the samples after higher temperature annealing have larger blue shifts, indicating heavier doping. This suggests that more adsorption sites are available for molecular adsorption after higher temperature annealing. The molecular doping not only happened in SLG; the Raman peaks of both bi- and multilayer graphenes show blue shifts after the annealing process and exposed to air ambient, but

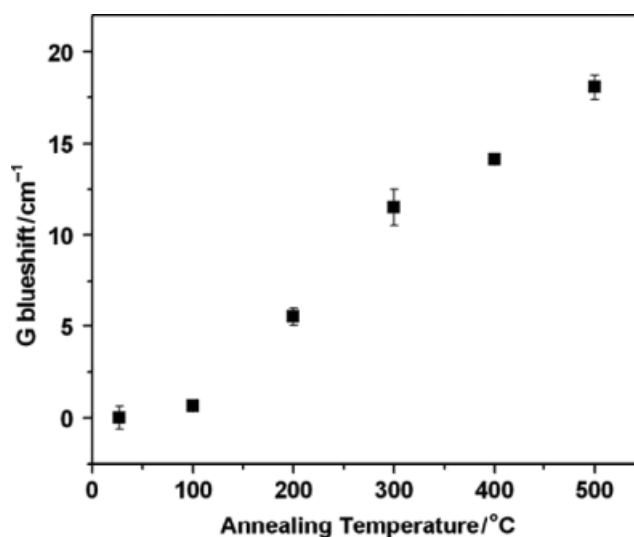


**Figure 3.** Blue shift of G band wavenumber of SLG after annealing at different temperatures and exposed to air ambient. The amount of blue shift on G band can be used to estimate the doping concentration.

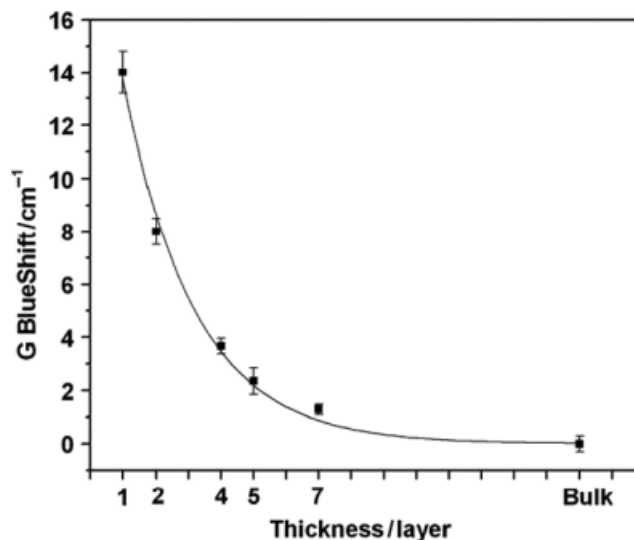


**Figure 4.** The amount of G band blue shifts of graphene with different thicknesses after annealed in 500 °C and exposed to air ambient. The black curve is a guide for the eye.

with smaller blue shifts for thicker samples. Figure 4 shows the G band blue shift as the graphene thickness increases after annealed at 500 °C and exposed to air ambient. It is obvious that with the increase of thickness, the shift decreases. For samples above seven layers and graphite, the blue shift can hardly be observed. This is because the doping has different effects on Raman features of graphene with different thicknesses.<sup>[15,29]</sup>

In order to experimentally verify the doping effect, we measured the transport properties of SLG before and after the vacuum annealing. Au/Ti ( $30 \times 10 \text{ nm}$ ) electrodes were directly evaporated on to a selected SLG flake by using a shield mask, as shown in the inset of Fig. 5. Figure 5 shows the resistance of graphene under different gate voltages. The highest resistance voltage indicates the neutral point of graphene. As we can see, the neutral point of graphene before annealing is at 2 V, indicating that the graphene

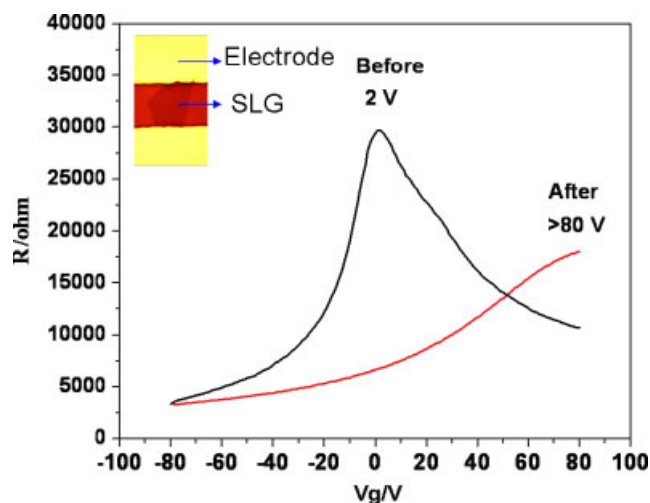


**Figure 5.** Transport properties of SLG (Resistance vs gate voltage) before annealing, after annealing and exposed to air ambient. The inset is optical image of SLG and two electrodes. The gate voltage corresponds to the highest resistance reveals the neutral point.

sample is only slightly (hole) p-doped. However, after annealing in vacuum at 300 °C for 2 h and exposing to air ambient, the neutral point shifts to more than 80 V. This clearly demonstrates that graphene is heavily p-doped after high-vacuum annealing and exposure to air ambient. By substituting the gate voltage into equation

$$n = CgVg/e \quad (1)$$

where  $Cg = 115 \text{ aF}/\mu\text{m}^2$ ,<sup>[15]</sup> the hole concentration of graphene after annealing and molecular adsorption is larger than  $5.8 \times 10^{12} \text{ cm}^{-2}$ . This corresponds to a G band blue shift of around  $10 \text{ cm}^{-1}$ ,<sup>[17]</sup> which agrees with the results shown in Fig. 3.

The molecular adsorption of graphene after vacuum annealing and the consequent induced heavy doping should be taken into consideration in the process of fabricating graphene-based electronic devices and gas sensors. To avoid such doping effect, the graphene samples should be annealed again in vacuum before fabrication. From another point of view, as the graphene sample is still of high quality after the molecular doping, this provides an easy and controllable technique to introduce heavy doping in graphene. The doping concentration can be remarkably increased ( $\sim 10^{13} \text{ cm}^{-2}$ ) after vacuum annealing compared to directly exposing graphene to a gas atmosphere ( $10^{10}$ – $10^{11} \text{ cm}^{-2}$ ).<sup>[8]</sup> Moreover, the doping concentration can be easily controlled by the annealing temperature, as shown in Fig. 3. Such an easy and efficient way to introduce and control the doping concentration in graphene would greatly help in its future application in nanoelectronic devices, such as controlling the channel type of graphene ribbon transistor and fabrication of graphene p–n junctions. It may also enhance the sensitivity of graphene gas sensor. Not only  $\text{O}_2$  and  $\text{H}_2\text{O}$  but other gases such as  $\text{NH}_3$ ,  $\text{NO}_2$ ,  $\text{CO}$ ,  $\text{NO}$ <sup>[11]</sup> can also be adsorbed on graphene after the vacuum annealing and introduce heavy electron/hole doping in graphene.

## Conclusion

In summary, we have demonstrated using Raman spectroscopy that graphene is heavily p-doped after vacuum annealing and exposure to air ambient. The doping is due to the adsorption of

$\text{H}_2\text{O}$  and  $\text{O}_2$  molecules on graphene, followed by charge transfer. The doping concentration is remarkably increased ( $\sim 10^{13} \text{ cm}^{-2}$ ) after vacuum annealing compared to directly exposing graphene to a gas atmosphere ( $10^{10}$ – $10^{11} \text{ cm}^{-2}$ ).<sup>[8]</sup> The doping effect is also demonstrated by transport measurements on SLG. Attention should be paid to this observation while fabricating graphene-based electronic devices. On the other hand, it also provides a practical and efficient way to introduce heavy doping in graphene. The quality of graphene still remains high after the doping process, confirmed by the absence of the defect-induced D band in the Raman spectrum. Moreover, the doping concentration can be controlled by the annealing temperature. We propose that graphene can also be exposed to other molecules after vacuum annealing, such as  $\text{NH}_3$ ,  $\text{NO}_2$ ,  $\text{CO}$ , to achieve electron/hole doping with different concentrations. Our results also help in a better understanding of how graphene properties are expected to change during the fabrication of devices, such as the annealing process, which would provide valuable information for device fabrication.

## References

- [1] K. S. Novoselov, A. K. Geim, S. V. Morozov, D. Jiang, Y. Zhang, S. V. Dubonos, I. V. Grigorieva, A. A. Firsov, *Science* **2004**, *306*, 666.
- [2] A. K. Geim, K. S. Novoselov, *Nat. Mater.* **2007**, *6*, 183.
- [3] J. Sabio, C. Seoanez, S. Fratini, F. Guinea, A. H. Castro, F. Sols, *Phys. Rev. B* **2008**, *77*, 195409.
- [4] X. Du, I. Skachko, A. Barker, E. Y. Andrei, *Nat. Nano* **2008**, *3*, 491.
- [5] E. J. H. Lee, K. Balasubramanian, R. T. Weitz, M. Burghard, K. Kern, *Nat. Nano* **2008**, *3*, 486.
- [6] L. DiCarlo, J. R. Williams, Y. M. Zhang, D. T. McClure, C. M. Marcus, *Phys. Rev. Lett.* **2008**, *100*, 156801.
- [7] T. O. Wehling, K. S. Novoselov, S. V. Morozov, E. E. Vdovin, M. I. Katsnelson, A. K. Geim, A. I. Lichtenstein, *Nano Lett.* **2008**, *8*, 173.
- [8] F. Schedin, A. K. Geim, S. V. Morozov, E. W. Hill, P. Blake, M. I. Katsnelson, K. S. Novoselov, *Nat. Mater.* **2007**, *6*, 652.
- [9] W. Chen, S. Chen, D. C. Qi, X. Y. Gao, A. T. S. Wee, *J. Am. Chem. Soc.* **2007**, *129*, 10418.
- [10] O. Leenaerts, B. Partoens, F. M. Peeters, *Appl. Phys. Lett.* **2008**, *92*, 243125.
- [11] O. Leenaerts, B. Partoens, F. M. Peeters, *Phys. Rev. B* **2008**, *77*, 125416.
- [12] S. Y. Zhou, D. A. Siegel, A. V. Fedorov, A. Lanzara, *Phys. Rev. Lett.* **2008**, *101*, 086402.
- [13] S. Reich, C. Thomsen, *Philos. Trans. R. Soc. A* **2004**, *362*, 2271.
- [14] M. A. Pimenta, G. Dresselhaus, M. S. Dresselhaus, L. G. Cancado, A. Jorio, R. Saito, *Phys. Chem. Chem. Phys.* **2007**, *9*, 1276.
- [15] J. Yan, Y. B. Zhang, P. Kim, A. Pinczuk, *Phys. Rev. Lett.* **2007**, *98*, 166802.
- [16] S. Pisana, M. Lazzeri, C. Casiraghi, K. S. Novoselov, A. K. Geim, A. C. Ferrari, F. Mauri, *Nat. Mater.* **2007**, *6*, 198.
- [17] A. Das, S. Pisana, B. Chakraborty, S. Piscanec, S. K. Saha, U. V. Waghmare, K. S. Novoselov, H. R. Krishnamurthy, A. K. Geim, A. C. Ferrari, A. K. Sood, *Nat. Nano* **2008**, *3*, 210.
- [18] Z. H. Ni, H. M. Wang, J. Kasim, H. M. Fan, T. Yu, Y. H. Wu, Y. P. Feng, Z. X. Shen, *Nano Lett.* **2007**, *7*, 2758.
- [19] Z. H. Ni, H. M. Fan, X. F. Fan, H. M. Wang, Z. Zheng, Y. P. Feng, Y. H. Wu, Z. X. Shen, *J. Raman Spectrosc.* **2007**, *38*, 1449.
- [20] I. Calizo, A. A. Balandin, W. Bao, F. Miao, C. N. Lau, *Nano Lett.* **2007**, *7*, 2645.
- [21] M. X. Gu, Y. C. Zhou, L. K. Pan, Z. Sun, S. Z. Wang, C. Q. Sun, *J. Appl. Phys.* **2007**, *102*, 083524.
- [22] Z. H. Ni, H. M. Wang, Y. Ma, J. Kasim, Y. H. Wu, Z. X. Shen, *ACS Nano* **2008**, *2*, 1033.
- [23] C. Casiraghi, S. Pisana, K. S. Novoselov, A. K. Geim, A. C. Ferrari, *Appl. Phys. Lett.* **2007**, *91*, 233108/1.
- [24] P. Ruoff, C. Lillo, *Biochem. Biophys. Res. Commun.* **1990**, *172*, 1000.
- [25] L. Freund, J. Halbritter, J. K. H. Horber, *Microsc. Res. Tech.* **1999**, *44*, 327.

- [26] J. C. Meyer, C. Kisielowski, R. Erni, M. D. Rossell, M. F. Crommie, A. Zettl, *Nano Lett.* **2008**, *8*, 3582.
- [27] T. J. Booth, P. Blake, R. R. Nair, D. Jiang, E. W. Hill, U. Bangert, A. Bleloch, M. Gass, K. S. Novoselov, M. I. Katsnelson, A. K. Geim, *Nano Lett.* **2008**, *8*, 2442.
- [28] L. Liu, S. M. Ryu, M. R. Tomasik, E. Stolyarova, N. Jung, M. S. Hybertsen, M. L. Steigerwald, L. E. Brus, G. W. Flynn, *Nano Lett.* **2008**, *8*, 1965.
- [29] J. Yan, E. A. Henriksen, P. Kim, A. Pinczuk, *Phys. Rev. Lett.* **2008**, *101*, 136804.